**Surface Chemistry**

# Water-Assisted Homolytic Dissociation of Propyne on a Reduced Ceria Surface

*Jian-Qiang Zhong,\* Zhong-Kang Han, Kristin Werner, Xiao-Yan Li, Yi Gao,*
*Shamil Shaikhutdinov, and Hans-Joachim Freund*

***Abstract:*** *The emergence of ceria ($CeO_2$) as an efficient catalyst for the selective hydrogenation of alkynes has attracted great attention. Intensive research effort has been devoted to understanding the underlying catalytic mechanism, in particular the $H_2$–$CeO_2$ interaction. Herein, we show that the adsorption of propyne ($C_3H_4$) on ceria, another key aspect in the hydrogenation of propyne to propene, strongly depends on the degree of reduction of the ceria surface and hydroxylation of the surface, as well as the presence of water. The dissociation of propyne and the formation of methylacetylide ($CH_3CC$-) have been identified through the combination of infrared reflection absorption spectroscopy (IRAS) and DFT calculations. We demonstrate that propyne undergoes heterolytic dissociation on the reduced ceria surface by forming a methylacetylide ion on the oxygen vacancy site and transferring a proton to the nearby oxygen site (OH group), while a water molecule that competes with the chemisorbed methylacetylide at the vacancy site assists the homolytic dissociation pathway by rebounding the methylacetylide to the nearby oxygen site.*

**C**eria ($CeO_2$) is a versatile material in heterogeneous catalysis as a result of its facile reducibility in terms of the oxidation and reduction of its cerium ions.[1] The discovery of the excellent catalytic performance of ceria in the selective hydrogenation of alkynes to alkenes opens new directions for the use of this oxide.[2] Pérez-Ramírez and co-workers first demonstrated that pure ceria exhibits excellent activity and selectivity in catalyzing the hydrogenation of propyne and ethyne to propene and ethene, respectively.[2,3] These counterintuitive findings triggered numerous experimental and

theoretical investigations into the mechanism of the selective hydrogenation of alkynes by ceria.[4]

Hydrogen activation on ceria is generally considered to be the main rate-limiting step since the optimal reaction conditions require a large $H_2$/alkyne ratio (30:1) and the conversion of alkyne increases as the $H_2$ partial pressure increases.[2–4] Extensive studies on the interaction of $H_2$ and ceria show that the dissociation of $H_2$ proceeds through a hydride intermediate.[5] Both oxygen vacancies and surface terminations of ceria play crucial roles in $H_2$ activation.[5a,c] The formation of surface and bulk hydride species upon $H_2$ adsorption at elevated temperatures was demonstrated by in situ inelastic neutron spectroscopy studies.[5b]

In contrast, the related activation of alkynes on ceria, another key aspect of the hydrogenation processes, are much less explored. Vilé et al. proposed that propyne ($C_3H_4$) dissociates through interactions with the strong acid/base sites (i.e. the cerium and oxygen atoms), ending up with a hydroxy and a methylacetylide ($CH_3CC$-) group on top of the Ce atom. The methylacetylide group is then hydrogenated by sequential addition of H atoms to produce propene ($C_3H_6$).[2] Cao et al. concluded that a π-bonded ethyne ($C_2H_2$) molecule at the oxygen site of ceria is the dominant active surface species for the hydrogenation reactions.[4c] However, these experimental studies were exclusively performed on powder samples. The complex surface morphology of powder samples renders such studies very difficult and somewhat uncertain. In contrast to metal surfaces, there are very few studies regarding the adsorption process of alkynes on metal oxides.[6] The adsorption sites, adsorption geometries, and detailed interactions are mostly unknown.

[*] Dr. J. Q. Zhong, Dr. K. Werner, Dr. S. Shaikhutdinov,
Prof. Dr. H.-J. Freund
Department of Chemical Physics
Fritz-Haber-Institut der Max-Planck-Gesellschaft
Faradayweg 4–6, 14195 Berlin (Germany)
E-mail: zhong@fhi-berlin.mpg.de
        zjq.txt@gmail.com

Dr. Z. K. Han
Theory Department
Fritz-Haber-Institut der Max-Planck-Gesellschaft
Faradayweg 4–6, 14195 Berlin (Germany)
and
Center for Energy Science and Technology
Skolkovo Institute of Science and Technology
143026 Moscow (Russia)

Dr. Z. K. Han, X. Y. Li, Prof. Y. Gao
Division of Interfacial Water and
Key Laboratory of Interfacial Physics and Technology

Shanghai Institute of Applied Physics
Chinese Academy of Sciences
201800 Shanghai (China)

Prof. Y. Gao
Zhangjiang Laboratory, Shanghai Advanced Research Institute
Chinese Academy of Sciences
201210 Shanghai (China)

Herein, well-ordered CeO$_2$(111) films were prepared as well-defined model systems to study alkyne activation on ceria surfaces. Detailed adsorption and activation processes of propyne on ceria surfaces have been clearly identified for the first time by using infrared reflection-absorption spectroscopy (IRAS) and density functional theory (DFT). It was found that propyne only physisorbs on a fully oxidized ceria surface, but chemisorbs on a reduced ceria surface through a heterolytic dissociation. However, traces of water may alter the dissociation mode towards homolytic. This effect may have a strong impact on the alkyne hydrogenation mechanism.

Both oxidized stoichiometric CeO$_2$(111) and reduced CeO$_{2-x}$(111) ceria films were fabricated on Ru(0001) substrates.[5c,7] The surface crystal structures and the electronic structures of these ceria films were characterized by low-energy electron diffraction (LEED) and X-ray photoelectron spectroscopy (XPS; Figure 1a–d). The reduced CeO$_{2-x}$(111) film showed a complex $(\sqrt{7} \times \sqrt{7})$-R19.1° LEED pattern formed by oxygen vacancies, which corresponds to a ι-Ce$_7$O$_{12}$ phase.[5c,8] The Ce 3d XP spectrum of CeO$_2$(111) showed characteristic peaks for Ce$^{4+}$, which were commonly described in terms of three doublets (Figure 1c).[5c,9] In CeO$_{2-x}$(111), additional XPS features appeared as a result of the oxygen vacancies. The dashed lines shown in Figure 1c show the characteristic peaks for a Ce$^{3+}$ state. The degree of surface reduction [Ce$^{3+}$/(Ce$^{4+}$ + Ce$^{3+}$)] is estimated to be around 20%, which is equivalent to about 10% of the oxygen sites being vacant (note that one oxygen vacancy creates two Ce$^{3+}$ ions).[5c,7] The weak signal at 531.8 eV in the O 1s XP spectrum of CeO$_{2-x}$(111) was previously attributed to the oxygen anions near the oxygen vacancy (Figure 1d).[10] However, surface hydroxy groups with similar binding energies caused by the adsorption of trace amounts of water cannot be fully excluded (Figure S1 in the Supporting Information).

The interaction between propyne and ceria was studied by IRAS. Propyne was precisely dosed onto the ceria surfaces with a calibrated molecular beam.[11] As shown in Figure 1e, four main features located at 1439 cm$^{-1}$, 2114 cm$^{-1}$, 2927 cm$^{-1}$, and 3263 cm$^{-1}$ appeared on CeO$_2$(111) after a dosage of 0.3 Langmuir (1 L = 10$^{-6}$ torr s) propyne at 120 K. In contrast, no vibrational modes were observed after exposure at room temperature, thus suggesting a weak adsorption of propyne on the fully oxidized O-terminated CeO$_2$(111) surface. On transition-metal surfaces, such as Cu(111),[12] Ni(111),[13] Pt(111),[14] and Rh(111),[15] propyne adsorbs molecularly with its C≡C axis lying essentially parallel to the metal surface, and with the methyl group and acetylenic hydrogen atom tilted away from the surface. Accordingly, we assign the vibrational bands to asymmetric deformation of the methyl group (1439 cm$^{-1}$) as well as C≡C stretch (2114 cm$^{-1}$), asymmetric and symmetric methyl stretches (2927 cm$^{-1}$, 2964 cm$^{-1}$), and acetylenic C−H stretch (3263 cm$^{-1}$) modes.

A strong band at 2039 cm$^{-1}$ was observed on a CeO$_{2-x}$(111) surface after exposure to either low and high temperatures (Figure 1e). At the same time, the acetylenic C−H stretch (3263 cm$^{-1}$) disappeared and a hydroxy feature
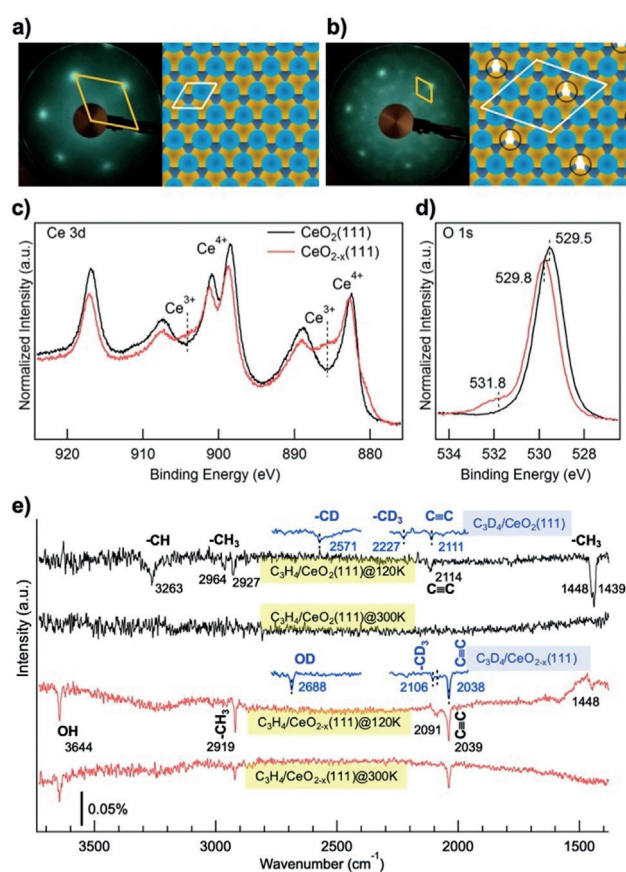


**Figure 1.** a,b) LEED patterns (at 100 eV) and schematic (top-view) structures of the oxidized CeO$_2$(111) film and the reduced CeO$_{2-x}$(111) film (Ce$_7$O$_{12}$, with a $\sqrt{7} \times \sqrt{7}$-R19.1° superstructure formed by oxygen vacancies). The light blue and dark blue balls represent the surface and subsurface O atoms, respectively, yellow balls represent the Ce atoms, black circles are the O vacancies, and the rhombuses represent the surface unit cells. c) Ce 3d and d) O 1s XP spectra of CeO$_2$(111) and CeO$_{2-x}$(111) films. The spectra were recorded in grazing emission mode to increase the surface sensitivity. e) IRAS of a 0.3 L dosage of propyne on CeO$_2$(111) and CeO$_{2-x}$ (111). The temperatures during the propyne exposure and IRAS measurements are indicated. IRAS of a 0.3 L dosage of D-substituted propyne (C$_3$D$_4$) on CeO$_2$(111) and CeO$_{2-x}$ (111) at 120 K are also shown in (e) (blue spectra).

arose at 3644 cm$^{-1}$, thus indicating cleavage of the acetylenic CH bond, that is, a dissociative chemisorption of propyne on CeO$_{2-x}$(111) to form a methylacetylide.

The strong vibrational mode at 2039 cm$^{-1}$ might also correspond to the related C≡C feature. Compared to that on CeO$_2$(111), the significantly weaker C≡C stretch is mainly attributed to its flat-lying configuration, which is IRAS inactive according to the surface selection rules.[16] The enhancement of the C≡C stretch band on CeO$_{2-x}$(111) suggests an upright configuration of the methylacetylide. The observed shift of the C≡C stretch to lower wavenumbers is an indication of its chemical bonding with the oxygen vacancy site. It should be noted that CeO$_{2-x}$(111) is reduced even further by the chemisorption of propyne (Figures S1 and S2).

This scenario is further supported by adsorption experiments with D-substituted propyne (C$_3$D$_4$; blue spectra in

Figure 1e). The appearance of the OD band (2688 cm$^{-1}$) and the enhancement of the C≡C band (2038 cm$^{-1}$) provide compelling evidence for the propyne dissociation resulting in an upright methylacetylide on the oxygen vacancies of CeO$_{2-x}$(111). The recombination desorption occurs at a temperature as high as 465 K, as found by temperature-programed desorption (TPD; Figure 2), thus suggesting the methylacetylide species has a high thermal stability.
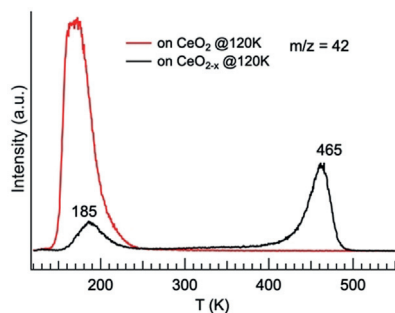


**Figure 2.** Propyne (C$_3$D$_4$) traces in TPD spectra. The spectra were recorded after exposure of CeO$_2$(111) and CeO$_{2-x}$(111) to 1 L C$_3$D$_4$ at 120 K. The heating rate was 2 K s$^{-1}$.

We use the C≡C stretch vibrational mode as a fingerprint to study the evolution of methylacetylide species upon the adsorption of water. The interactions between propyne and water were investigated in two comparative experiments: 1) propyne on a CeO$_{2-x}$(111) surface with preadsorbed water, and 2) water on a CeO$_{2-x}$(111) surface with preadsorbed propyne. We find that water can dissociate on the oxygen vacancy of the CeO$_{2-x}$(111) surface to form hydroxy groups.

Figure 3a shows how we firstly dosed 0.1 L D$_2$O onto CeO$_{2-x}$(111), followed by dosing 0.3 L of propyne. The band at 2686 cm$^{-1}$ is the hydroxy group formed by the dissociation of D$_2$O. The distinguishable C≡C band suggests that propyne can still chemisorb on this surface. However, there is no propyne chemisorption once all the oxygen vacancies are occupied at the increased D$_2$O dosage of 0.3 L. These results demonstrate that water and propyne compete for the same chemisorption sites, namely, the oxygen vacancy.

In contrast, water can further dissociate even if the oxygen vacancies are already occupied by the chemisorbed propyne (Figure 3b). The C≡C band at 2039 cm$^{-1}$ slightly decreases and a new band at 2166 cm$^{-1}$ arises upon the adsorption of D$_2$O. The transformation becomes apparent when the temperature is increased from 300 K to 500 K. The band at 2039 cm$^{-1}$ disappears while the band at 2166 cm$^{-1}$ increases in intensity. In addition, the band corresponding to the hydroxy group shifts by about 10 cm$^{-1}$ to a higher frequency compared to that on clean CeO$_{2-x}$(111) (i.e. 2695 cm$^{-1}$ versus 2686 cm$^{-1}$). These findings indicate that methylacetylide interacts with water molecules, and it should be noted that the methyl stretching band (2919 cm$^{-1}$) was slightly affected by the adsorption of water.

DFT calculations were carried out to rationalize the experimental results and get more insight into the adsorption of propyne, in particular to understand the effect of water on the preadsorbed propyne. For slightly reduced CeO$_{2-x}$(111),
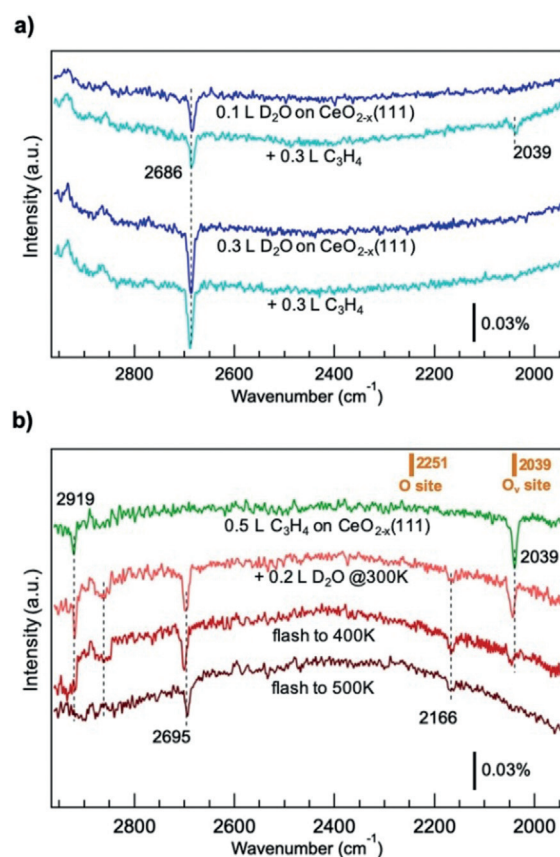


**Figure 3.** a) IRAS of propyne adsorption on a CeO$_{2-x}$(111) surface with preadsorbed water at 400 K. Top two spectra: 0.3 L C$_3$H$_4$ on 0.1 L D$_2$O/ CeO$_{2-x}$(111) (oxygen vacancies are partially occupied by water); bottom two spectra: 0.3 L C$_3$H$_4$ on 0.3 L D$_2$O/CeO$_{2-x}$(111) (oxygen vacancies are all occupied by water). b) IRAS of water adsorption on a CeO$_{2-x}$(111) surface with preadsorbed propyne. Propyne and water were dosed at 300 K, and then the sample was heated to the temperatures indicated. IRAS spectra were taken at 300 K. The two vertical bars are DFT-calculated vibrational frequencies for the C≡C bands (methylacetylide) on an oxygen vacancy site and oxygen site, respectively.

the oxygen vacancies are isolated, and the vacancies are, in fact, more stable in subsurface layers than on the surface.[17] As the number of oxygen vacancies increases, some ordered patterns or clusters of oxygen vacancies may be formed.[18] In our DFT studies, we made use of a well-ordered reduced CeO$_{2-x}$(111) with a $(\sqrt{7} \times \sqrt{7})$-R19.1° superstructure, as in Ref. [5c]. As shown in Figure 4a, the most stable adsorption site for H$_2$O is on top of the oxygen vacancy, with one hydrogen atom binding to the nearby surface oxygen and another hydrogen atom pointing away from the surface. The adsorption energy is −0.75 eV, in good agreement with previous calculations.[19] By overcoming a very small activation energy barrier of 0.12 eV, H$_2$O dissociates and forms two hydroxy groups, one of which fills the oxygen vacancy. The dissociation process is highly exothermic with a total reaction energy of 2.1 eV,[20] thus resulting in the strong adsorption of water on reduced ceria.[19a]

The oxygen vacancy also shows a high reactivity for propyne. According to our DFT calculations, propyne dissociates on the vacancy site in a straightforward manner with
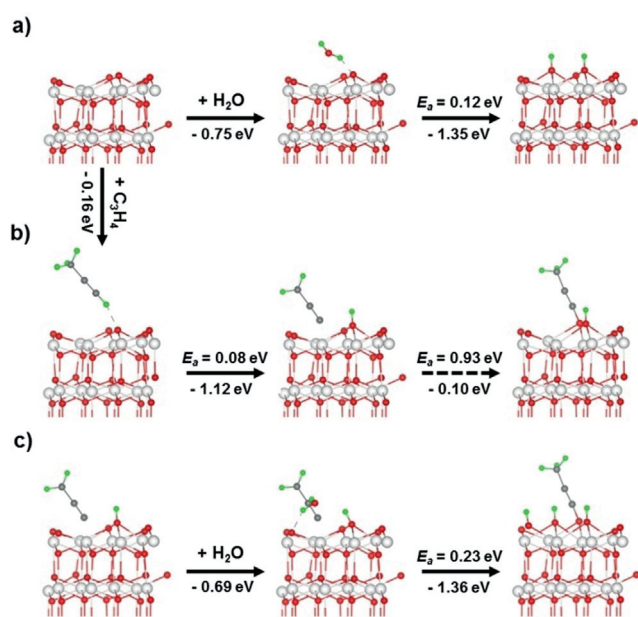
a)

b)

c)

**Figure 4.** Reaction pathway of the water-assisted homolytic dissociation of propyne on a reduced ceria surface. a) $H_2O$ dissociation on the oxygen vacancy site of $CeO_{2-x}$ (i.e. $Ce_7O_{12}$). b) Heterolytic dissociation of $C_3H_4$ on the oxygen vacancy site of $Ce_7O_{12}$. The transformation from heterolytic dissociation to homolytic dissociation is also indicated by the dashed arrow. c) Water-assisted homolytic dissociation of $C_3H_4$ on $Ce_7O_{12}$. The Ce, O, C, and H atoms are shown in white, red, gray, and green, respectively. $E_a$ is the energy barrier. The values under the arrows are the reaction energies.

an energy barrier of only 0.08 eV (Figure 4b). Cleavage of the CH bond results in one methylacetylide bonding to the vacancy site and one hydrogen atom bonded to the nearby oxygen atom to form a hydroxy group. This heterolytic dissociation of propyne on reduced ceria is exothermic, with a total reaction energy of 1.22 eV. We have also examined the possibility of the homolytic dissociation of propyne. It was found that the homolytic process has a much higher energy barrier, namely, 0.93 eV. However, the barrier can be significantly reduced (to 0.23 eV) by the presence of a water molecule (Figure 4c). In contrast, the coadsorption of propyne with a water molecule on an oxidized ceria surface does not reduce the energy barrier considerably for the dissociative adsorption of propyne. The interaction of the water molecule with the chemisorbed methylacetylide leads to the shift of the methylacetylide from the oxygen vacancy site to the nearby oxygen site. The calculated vibrational frequencies of the $C\equiv C$ bands are 2039 cm$^{-1}$ for methylacetylide on an oxygen vacancy site and 2251 cm$^{-1}$ for methylacetylide on an oxygen site, in fairly good agreement with the experimental observations (Figure 3b and Figure S4). As a result, the chemisorption of propyne proceeds through a homolytic dissociation under the assistance of a water molecule.

It is generally accepted that the hydrogenation reactions follow a Horiuti–Polanyi mechanism.[21] Accordingly, methylacetylide is considered as a reaction intermediate that is selectively hydrogenated by the sequential addition of H atoms to produce propene. The activation energy for $H_2$ dissociation on oxidized ceria surfaces ranges from 0.78 eV to 1.21 eV,[5c,d] which is smaller than that for the activation of

propyne (1.29 eV, Figure S5). Therefore, the adsorption of propyne seems to be the rate-limiting step on fully oxidized $CeO_2(111)$ surfaces. However, on $CeO_{2-x}(111)$ surfaces, propyne activation is much easier than hydrogen activation.

In our experiments, we do not observe $H_2$ dissociation on either $CeO_2(111)$ or $CeO_{2-x}(111)$ surfaces over a wide temperature range (100 K−500 K) at low $H_2$ pressures ($<10^{-6}$ mbar). However, $H_2$ dissociation occurs on reduced $CeO_{2-x}$ at higher pressure ($>10$ mbar), which is accompanied by hydride formation in the bulk.[5b,c,22] Nonetheless, water adsorption in our experiments results in hydroxy species similar to those formed on ceria upon interaction with hydrogen at high pressures.[5c] Therefore, the coadsorption of water and propyne in our experiments mimics the proposed reaction intermediates formed during hydrogenation reactions of propyne on $CeO_2(111)$ in the presence of excess hydrogen. Upon heating, the adsorbed hydroxy and methylacetylide species desorb as propyne and water in TPD experiments. Our molecular beam studies (not shown), which focus two beams of $H_2$ and propyne onto the ceria surfaces, did not show hydrogenated products. It appears that the reaction needs much higher pressures, such as those used for powder catalysts.[2] Further reactivity studies of this hydrogenation reaction on well-defined model systems remain to be done.

In summary, our experimental and computational results demonstrate that propyne weakly adsorbs on an oxidized ceria surface, while it dissociates at the oxygen vacancy sites of the reduced ceria surface through a heterolytic pathway. In the presence of a water molecule, the propyne adsorption becomes a homolytic dissociation. These results may aid in our understanding of the selective hydrogenation of alkynes on ceria.

### Experimental Section

Experiments were carried out in two UHV systems with background pressures of ca. $2\times10^{-10}$ mbar. The first system combines molecular beam techniques and an IRAS spectrometer (Bruker IFS66v/S). The second system combines an IRAS spectrometer (Bruker IFS66v/S) and XPS (Specs XR 50, PHOIBOS 150). In addition, both systems are equipped with LEED. Adsorption studies were performed with calibrated molecular beams or precisely controlled leak valves at various temperatures, as indicated in the text and figure captions.

The $CeO_2(111)$ film with a thickness of about 5 nm was grown on a Ru(0001) single crystal. Briefly, the Ru(0001) surface was cleaned with cycles of Ar$^+$ sputtering and annealing at 1200 K. It was then exposed to $1\times10^{-6}$ mbar $O_2$ at 1000 K to form a $3O(2\times2)$-Ru(0001) structure. Ce (99.9%, Sigma–Aldrich) was vapor-deposited onto the $3O(2\times2)$-Ru(0001) surface in $1\times10^{-6}$ mbar $O_2$. Proper wetting of the substrate was ensured by depositing the first few layers at a sample temperature of 120 K. Then, the temperature was raised to 673 K at a rate of 1 K s$^{-1}$ (while keeping the Ce flux) and kept constant during the deposition of the next layers. Deposition at 673 K was performed in cycles, including 30 to 60 min of Ce evaporation and subsequent annealing in $10^{-6}$ mbar $O_2$ at 1000 K for several minutes to ensure good film ordering. A reduced $CeO_{2-x}(111)$ film was prepared by annealing the $CeO_2(111)$ film at 1000–1200 K for 10–40 min in an ultrahigh vacuum. This film showed a $(\sqrt{7}\times\sqrt{7})$-R19.1° superstructure.

Spin-polarized DFT calculations were carried out using the generalized gradient approximation (GGA) of Perdew-Burke-Ernzerhof (PBE), as implemented in the VASP code.[23] The DFT+U method[24] with an effective U value of 5.0 eV was used to describe the localized Ce 4f states (Ce$^{3+}$), which is within the range of suitable values to describe reduced ceria-based systems.[25] Density functional perturbation theory–linear response calculations were performed to obtain the vibrational properties.[26]

## Conflict of interest

The authors declare no conflict of interest.

[1] A. Trovarelli, P. Fornasiero, *Catalysis by Ceria and Related Materials*, World Scientific, Sinapore, **2013**.

[2] G. Vilé, B. Bridier, J. Wichert, J. Pérez-Ramírez, *Angew. Chem. Int. Ed.* **2012**, *51*, 8620–8623; *Angew. Chem.* **2012**, *124*, 8748–8751.

[3] G. Vilé, S. Colussi, F. Krumeich, A. Trovarelli, J. Pérez-Ramírez, *Angew. Chem. Int. Ed.* **2014**, *53*, 12069–12072; *Angew. Chem.* **2014**, *126*, 12265–12268.

[4] a) J. Carrasco, G. Vilé, D. Fernández-Torre, R. Pérez, J. Pérez-Ramírez, M. V. Ganduglia-Pirovano, *J. Phys. Chem. C* **2014**, *118*, 5352–5360; b) M. García-Melchor, L. Bellarosa, N. López, *ACS Catal.* **2014**, *4*, 4015–4020; c) T. Cao, R. You, X. Zhang, S. Chen, D. Li, Z. Zhang, W. Huang, *Phys. Chem. Chem. Phys.* **2018**, *20*, 9659–9670; d) C. Riley, S. Zhou, D. Kunwar, A. De La Riva, E. Peterson, R. Payne, L. Gao, S. Lin, H. Guo, A. Datye, *J. Am. Chem. Soc.* **2018**, *140*, 12964–12973.

[5] a) O. Matz, M. Calatayud, *ACS Omega* **2018**, *3*, 16063–16073; b) Z. Wu, Y. Cheng, F. Tao, L. Daemen, G. S. Foo, L. Nguyen, X. Zhang, A. Beste, A. J. Ramirez-Cuesta, *J. Am. Chem. Soc.* **2017**, *139*, 9721–9727; c) K. Werner, X. Weng, F. Calaza, M. Sterrer, T. Kropp, J. Paier, J. Sauer, M. Wilde, K. Fukutani, S. Shaikhutdinov, H.-J. Freund, *J. Am. Chem. Soc.* **2017**, *139*, 17608–17616; d) M. García-Melchor, N. López, *J. Phys. Chem. C* **2014**, *118*, 10921–10926.

[6] A. V. Ivanov, A. E. Koklin, E. B. Uvarova, L. M. Kustov, *Phys. Chem. Chem. Phys.* **2003**, *5*, 4718–4723.

[7] Z. Li, K. Werner, K. Qian, R. You, A. Płucienik, A. Jia, L. Wu, L. Zhang, H. Pan, H. Kuhlenbeck, S. Shaikhutdinov, W. Huang, H.-J. Freund, *Angew. Chem. Int. Ed.* **2019**, *58*, 14686–14693; *Angew. Chem.* **2019**, *131*, 14828–14835.

[8] a) F. Dvořák, L. Szabová, V. Johánek, M. Farnesi Camellone, V. Stetsovych, M. Vorokhta, A. Tovt, T. Skála, I. Matolínová, Y. Tateyama, J. Mysliveček, S. Fabris, V. Matolín, *ACS Catal.* **2018**, *8*, 4354–4363; b) R. Olbrich, G. E. Murgida, V. Ferrari, C. Barth, A. M. Llois, M. Reichling, M. V. Ganduglia-Pirovano, *J. Phys. Chem. C* **2017**, *121*, 6844–6851; c) T. Duchoň, F. Dvořák, M. Aulická, V. Stetsovych, M. Vorokhta, D. Mazur, K. Veltruská, T. Skála, J. Mysliveček, I. Matolínová, V. Matolín, *J. Phys. Chem. C* **2014**, *118*, 357–365.

[9] D. R. Mullins, *Surf. Sci. Rep.* **2015**, *70*, 42–85.

[10] a) C. Yang, X. Yu, S. Heißler, A. Nefedov, S. Colussi, J. Llorca, A. Trovarelli, Y. Wang, C. Wöll, *Angew. Chem. Int. Ed.* **2017**, *56*, 375–379; *Angew. Chem.* **2017**, *129*, 382–387; b) V. Stetsovych, F. Pagliuca, F. Dvořák, T. Duchoň, M. Vorokhta, M. Aulická, J. Lachnitt, S. Schernich, I. Matolínová, K. Veltruská, T. Skála, D. Mazur, J. Mysliveček, J. Libuda, V. Matolín, *J. Phys. Chem. Lett.* **2013**, *4*, 866–871.

[11] J. Libuda, I. Meusel, J. Hartmann, H.-J. Freund, *Rev. Sci. Instrum.* **2000**, *71*, 4395–4408.

[12] a) M. A. Chesters, E. M. McCash, *J. Electron Spectrosc. Relat. Phenom.* **1987**, *44*, 99–108; b) A. Valcárcel, J. M. Ricart, F. Illas, A. Clotet, *J. Phys. Chem. B* **2004**, *108*, 18297–18305; c) R. L. Toomes, R. Lindsay, P. Baumgärtel, R. Terborg, J.-T. Hoeft, A. Koebbel, O. Schaff, M. Polcik, J. Robinson, D. P. Woodruff, A. M. Bradshaw, R. M. Lambert, *J. Chem. Phys.* **2000**, *112*, 7591–7599.

[13] A. J. Roberts, S. Haq, R. Raval, *J. Chem. Soc. Faraday Trans.* **1996**, *92*, 4823–4827.

[14] J. W. Peck, D. I. Mahon, B. E. Koel, *Surf. Sci.* **1998**, *410*, 200–213.

[15] a) B. E. Bent, C. M. Mate, J. E. Crowell, B. E. Koel, G. A. Somorjai, *J. Phys. Chem.* **1987**, *91*, 1493–1502; b) A. Valcárcel, A. Clotet, F. Illas, J. M. Ricart, *Phys. Chem. Chem. Phys.* **2007**, *9*, 311–317.

[16] K. Mudiyanselage, D. J. Stacchiola in *In-situ Characterization of Heterogeneous Catalysts* (Eds.: J. A. Rodriguez, J. C. Hanson, P. J. Chupas), John Wiley & Sons, Inc., Hoboken, New Jersey, **2013**, pp. 209–239.

[17] a) M. V. Ganduglia-Pirovano, J. L. F. Da Silva, J. Sauer, *Phys. Rev. Lett.* **2009**, *102*, 026101; b) F. Esch, S. Fabris, L. Zhou, T. Montini, C. Africh, P. Fornasiero, G. Comelli, R. Rosei, *Science* **2005**, *309*, 752–755.

[18] a) Z.-K. Han, Y.-Z. Yang, B. Zhu, M. V. Ganduglia-Pirovano, Y. Gao, *Phys. Rev. Mater.* **2018**, *2*, 035802; b) G. E. Murgida, V. Ferrari, A. M. Llois, M. V. Ganduglia-Pirovano, *Phys. Rev. Mater.* **2018**, *2*, 083609.

[19] a) H. A. Hansen, C. Wolverton, *J. Phys. Chem. C* **2014**, *118*, 27402–27414; b) M. B. Watkins, A. S. Foster, A. L. Shluger, *J. Phys. Chem. C* **2007**, *111*, 15337–15341.

[20] Z. Yang, Q. Wang, S. Wei, D. Ma, Q. Sun, *J. Phys. Chem. C* **2010**, *114*, 14891–14899.

[21] I. Horiuti, M. Polanyi, *Trans. Faraday Soc.* **1934**, *30*, 1164–1172.

[22] X. Li, J. Paier, J. Sauer, *arXiv e-prints* **2019**, https://doi.org/https://arxiv.org/abs/1904.13200.

[23] a) J. P. Perdew, K. Burke, M. Ernzerhof, *Phys. Rev. Lett.* **1996**, *77*, 3865–3868; b) G. Kresse, J. Furthmüller, *Phys. Rev. B* **1996**, *54*, 11169–11186; c) M. Cococcioni, S. de Gironcoli, *Phys. Rev. B* **2005**, *71*, 035105.

[24] S. L. Dudarev, G. A. Botton, S. Y. Savrasov, C. J. Humphreys, A. P. Sutton, *Phys. Rev. B* **1998**, *57*, 1505–1509.

[25] C. W. M. Castleton, J. Kullgren, K. Hermansson, *J. Chem. Phys.* **2007**, *127*, 244704.

[26] S. Baroni, S. de Gironcoli, A. Dal Corso, P. Giannozzi, *Rev. Mod. Phys.* **2001**, *73*, 515–562.